

Dynamical structures in binary media of potassium-driven neurons

D. E. Postnov¹, F. Müller², R. B. Schuppner², and L. Schimansky-Geier²

¹*Department of Physics, Saratov State University,
Astrakhanskaya ul. 83, Saratov 410012, Russia.*

²*Institute of Physics, Humboldt-University at Berlin,
Newtonstr. 15, D-12489 Berlin, FR Germany*

Abstract

According to the conventional approach neural ensembles are modeled with fixed ionic concentrations in the extracellular environment. However, in some cases the extracellular concentration of potassium ions can not be regarded as constant. That represents specific chemical pathway for neurons to interact and can influence strongly the behavior of single neurons and of large ensembles. The released chemical agent diffuses in the external medium and lowers thresholds of individual excitable units. We address this problem by studying simplified excitable units given by a modified FitzHugh-Nagumo dynamics. In our model the neurons interact only chemically via the released and diffusing potassium in the surrounding non-active medium and are permanently affected by noise. First we study the dynamics of a single excitable unit embedded in the extracellular matter. That leads to a number of noise-induced effects, like self-modulation of firing rate in an individual neuron. After the consideration of two coupled neurons we consider the spatially extended situation. By holding parameters of the neuron fixed various patterns appear ranging from spirals and traveling waves to oscillons and inverted structures depending on the parameters of the medium.

PACS numbers: 05.40.-a, 87.19.L-, 89.75.Kd

I. INTRODUCTION

According to a conventional view on neuronal dynamics, the electrical activity of a cell is represented by depolarization of its membrane potential. It is well described by the famous Hodgkin-Huxley model [1] describing the dynamics of the different ion channels and the gating ions. But also simplified model systems were introduced using less number of variables and control parameters [2] and are able to specify the many aspects of neuronal dynamics. Among them, the FitzHugh-Nagumo model [3] with a few control parameters plays the role of popular paradigm for many excitable systems. Due to its simplicity it helps a lot that ideas, which have been developed in neuronal dynamics, can be transferred to related problems of other nonlinear dynamics [4].

But an inevitable assumption and simplification have been made for these prototypical neuron models in terms of ionic currents. For example, it was assumed that in spite of transmembrane currents, both extracellular and intra-cellular ionic concentrations remain unchanged during depolarizations. Such a simplification is natural and acceptable if one considers individual neurons or segments of an excitable medium during a sufficiently short course of firing.

However, in other cases it will be not realistic. For example, there is the experimental evidence that extracellular concentration of potassium ions can vary significantly during the course of intensive neuronal firings [5, 6]. The detailed modeling of what happens during the course of ischemia shows the strong increase of extracellular potassium concentration up to 80 mM [7, 8, 9, 10, 11]. The glial cells, surrounding and supporting neurons, activate the potassium pumping when its concentration rise considerably (more then twice in medical leech) [12]. This excessive elevation of potassium concentration is considered to be an important element of mechanism of epileptic seizure development [13, 14]. As the relevant computational studies, early modeling attempts were focused mostly on mechanisms of extracellular potassium clearance and showed that pathways different from diffusion must be involved in this process [15, 16, 17, 18]. More recent models addressed the detailed neuronal morphology [19, 20] or the role of specific ion channels in formation of self-sustained bursting behavior [13, 21]. It was also shown that the interplay between ion concentrations and neural activity can lead to self-sustained pathological neural activation even in the case of an isolated cell. The wider list of modeling issues on topic was recently reviewed in [22].

While the effects of variable ionic concentration are embedded in the quantitative high-dimensional models, it is difficult to distinguish them from the other aspects of system behavior. At the same time, the set of frequently used simplified models does not cover the problem, just not having the appropriate control parameters.

One of the authors addressed this problem in recent works [23, 24], where the effects of potassium mediated coupling were investigated using the Hodgkin-Huxley type model of leech neurons. It was shown, that such rather simplified, but still quantitative model reproduces the main features of small ensembles of potassium-driven neurons.

However, to study the behavior of large networks by means of a quantitative model, one need to introduce the number of control parameters that are difficult to estimate or just unknown. The alternative way is to develop a simplified non-dimensional model that can capture at a qualitative level the specific features of potassium-coupled neurons and allows one to build the large networks using reasonable set of control parameters.

In the present work we derive such a model in the form of an extended FitzHugh-Nagumo (FHN) system [3] with an additional equation describing the dynamics of extracellular potassium. Since our model inherits the key features of a FHN neuron, it is physically transparent and tractable and thus provides the better chance to learn more about nonlinear mechanisms governing the formation of spatio-temporal patterns in large networks. On the other hand, compared to a leaky integrate and fire models (LIF) the FHN includes the reset mechanism of the neuron. Several states and according dynamic behavior which we will observe later on in the article refer to the excited state of the FHN and which is not part of a LIF [25, 26].

Applied to interacting neurons we assume that the interaction of neurons is restricted to the single chemical pathway. Coupling takes place indirectly due to the potassium concentration outside the cells, only. Although there is no explicit distance defined in the extended model, the neurons are strictly separated and a direct contact of the action potentials is excluded. Therefore the transport of activity through the heterogeneous medium of neurons and exterior is slower than in a homogeneous excitable medium.

The patterns appearing in the two-dimensional system show phenomena, which are reminiscent of chemical experiments in which comparable heterogeneous situations like two-layer systems or chemical oscillators moving in a diffusive environment have been studied [27, 28]. Also some of the presented structures relate to studies on the Ca^{2+} release across endoplasmic reticulum [29, 30], where clusters of with a finite number ion channels on the

recituculum take over the role of the noisy excitable neurons and Ca^{2+} diffuses freely in the cytoplasm.

In our work we attempt to classify the observed spatio-temporal patterns according to the relation between the key control parameters of the extracellular medium. The most noticeable behavior are randomly-walking spots, long living meandering excitations, anti-phase firing patterns and inverted spirals and waves.

II. MINIMAL MODEL FOR A POTASSIUM-DRIVEN NEURON

A. Background

We consider an environment which is schematically depicted in Fig. 1 (a). We assume that there is a certain volume between the cells from which the ionic exchange with the outer bath is rate limited. For simplicity we assume that this volume is homogeneous and denote the potassium concentration here as $[K^+]_e$.

With time, particularly during firing events in neurons, the potassium channels $*1*$ in its membranes become open and outward currents from the cells deliver potassium to the extracellular space. Thus, $[K^+]_e$ rises while the inter-cellular potassium concentration $[K^+]_i$ decreases just slightly, because $[K^+]_i \gg [K^+]_e$. In fact, one can neglect the associated intracellular changes of the potassium concentration and assume that this concentration remains constant.

$Na - K$ At-Pase $*2*$ pumps K^+ back into the cells. This uptake is balanced by the leakage when the potassium concentration is at equilibrium value $[K^+]_0$. The exchange of K^+ ions with a surrounding bath is assumed to take place by a diffusion process, hence governed by the concentration difference between the exterior and the bath. Assuming the bath potassium concentration to be equal $[K^+]_0$, one can simplify the description of the process by incorporating all potassium uptake processes in an effective diffusion rate parameter γ .

Then the balance of potassium concentration in the inter-cellular space $[K^+]_e$ can be

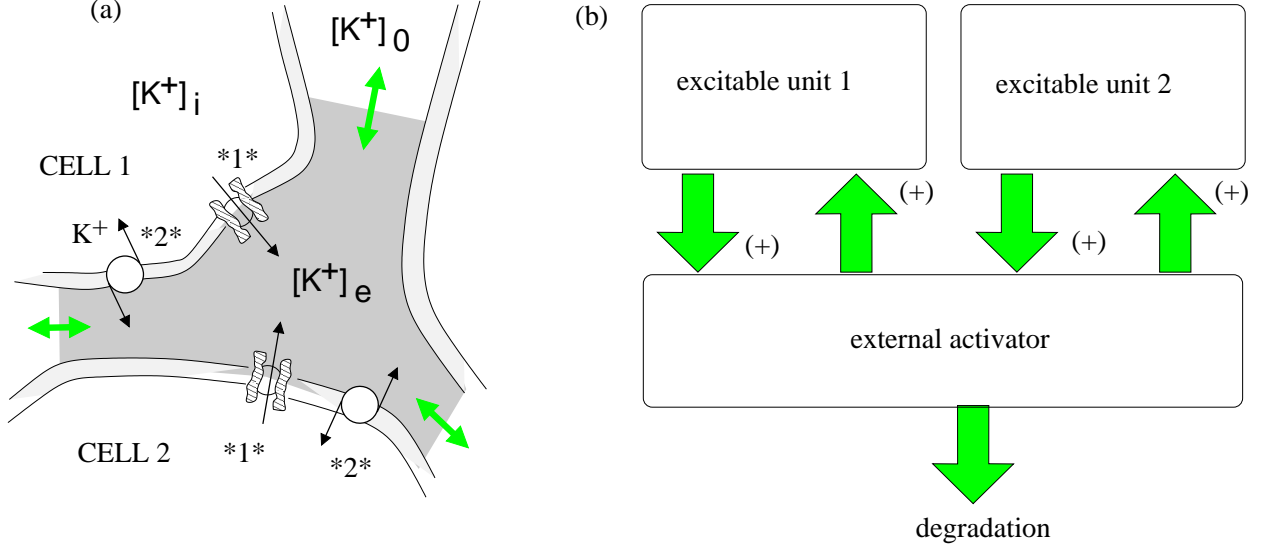


FIG. 1: (Color online) (a) Schematic representation of the potassium signaling pathways between closely located cells, (b) the corresponding structure of the functional model.

described as following:

$$W \frac{d[K^+]_e}{dt} = \frac{1}{F} \sum_{i=1}^N I_{i,K} + \gamma([K^+]_0 - [K^+]_e), \quad (1)$$

where W is the extracellular volume per unit area of the membrane, N the total number of cells being neighbors to this volume, $I_{i,K}$ is the electric potassium current per unit area from the i th-cell which is divided by Faraday's constant F to provide the ion flow. The second term $\gamma([K^+]_0 - [K^+]_e)$ describes the effective diffusion of potassium to and from the bath. This balance equation (1) provides the basis for the qualitative description in terms of a functional model we will introduce below.

Note, the variation of the ratio between the extra- and intra-cellular potassium concentrations affects the corresponding (Nernst-) potential and, hence, the firing activity. The considerable rise of extracellular potassium concentration depolarizes the cell and can evoke the transition to spontaneous firing. However, too high extracellular potassium concentration becomes toxic and can block the cell activity, completely.

B. Model

In this subsection we propose a functional model that aims the qualitative reproduction of main effects arising if a variable extracellular potassium concentration is taken into account. The structure of the model is schematically depicted in Fig. 1 (b). Namely, several excitable units standing for a number of neurons contribute to the extracellular potassium increase. This “external activator” stands for the inter-cellular space between the cells with variable potassium concentration. It is (i) activated during a high-level state of one of the excitable units, (ii) provides an additional stimulus to the excitable units and (iii) relaxes to an equilibrium when receives no activation.

Let us first confine to a single neuron interacting with the external medium. Particularly we will implement the activity of the excitable neuron by the FitzHugh-Nagumo (FHN) system [2, 3]. Therefore we assume that the gating of potassium release of a single neuron is given by

$$\varepsilon \dot{x} = x - x^3/3 - y, \quad (2)$$

$$\tau(x)\dot{y} = x + a - Cz, \quad (3)$$

where ε controls the time scale separation of the fast activator x and the slow inhibitor y . The operating regime of the FHN neuron is defined by a , playing the role similar to the applied current in ionic currents-based neuron models. We assume that it may fluctuate around some mean value a_0 :

$$a = a_0 + \sqrt{2D}\xi(t), \quad (4)$$

where $\xi(t)$ is white Gaussian noise with zero mean and intensity D .

An additional time scale $\tau(x)$ in (3) is introduced in order to control the two time scales independently, associated with firing (high level of x variable) and refractory state (low level of x) which will gain importance in our problem. Specifically, we introduce the sigmoidal function

$$\Psi(x) = \frac{1}{2} \left(1 + \tanh \left(\frac{x}{x_s} \right) \right), \quad (5)$$

which is sensitive to the current value of the x variable: it tends to zero for $x \ll 0$, and to one if $x \gg 0$, while x_s scales the transition between these states. Actually, we use (5) as a smooth replacement of a Heaviside function to distinguish between the excited and the

resting states of the FHN neuron. With Eq.(5) $\tau(x)$ shapes as

$$\tau(x) = \tau_l + (\tau_r - \tau_l)\Psi(x). \quad (6)$$

and takes values τ_l and τ_r in the rest and excited states, respectively.

We label the variable dimensionless extracellular potassium concentration by $z(t) \geq 0$. Its dynamics is given in accordance with Eq.(1) by

$$\dot{z} = \alpha g(x) - \beta z. \quad (7)$$

with $z = z^0 = 0$ corresponding to the steady concentration $[K^+]_0$ and β is the rate of ion losses. Respectively the parameters α stands for the summary ionic fluxes outward the cells. It scales inversely as well to the size of the extracellular volume. These fluxes are released into the exterior for high x values if the cell is excited and channels are open ($x \approx 2$). They disappear in the rest state $x \approx -1$, if channels are closed. Hence likewise for the time scales we are able to use the function Eq.(5) as switcher in Eq.(7). Hence we will set $g(x) = \Psi(x)$.

The value of z enters in (3) with a factor C . It represents the depolarizing effect of the increased extracellular concentration. For a given non vanishing value of z it results in an additional shift of the y -nullcline decreasing effectively the excitability value a . Mathematically we can call it a second activator which was previously introduced in models for nonlinear semiconductors [31].

The set of equations described above is dimensionless and, therefore, the relationship to ionic current-based neuronal models can be only qualitative. However, for the sake of simplicity and to keep the connection with the original problem, we will use the terminology from neurophysiology further on in order to describe the dynamic behavior of the model as well as the meaning of control parameters. In the following we refer to system (2)-(7) as the FHN-K model.

For the numeric simulation the following values of control parameter values were used: $\varepsilon = 0.04$, $a_0 = 1.04$, $C = 0.0 \dots 0.1$, $\alpha = 1.0 \dots 12.0$, $\beta = 0.05 \dots 0.5$, $x_0 = 0.0$, $x_s = 0.2$, $\tau_l = 1.0 \dots 10.0$, $\tau_r = 1.0$. It sets the neuron without the regulation by external potassium ($C = 0$) in an excitable regime.

C. Nullclines and fixed points of the single unit model

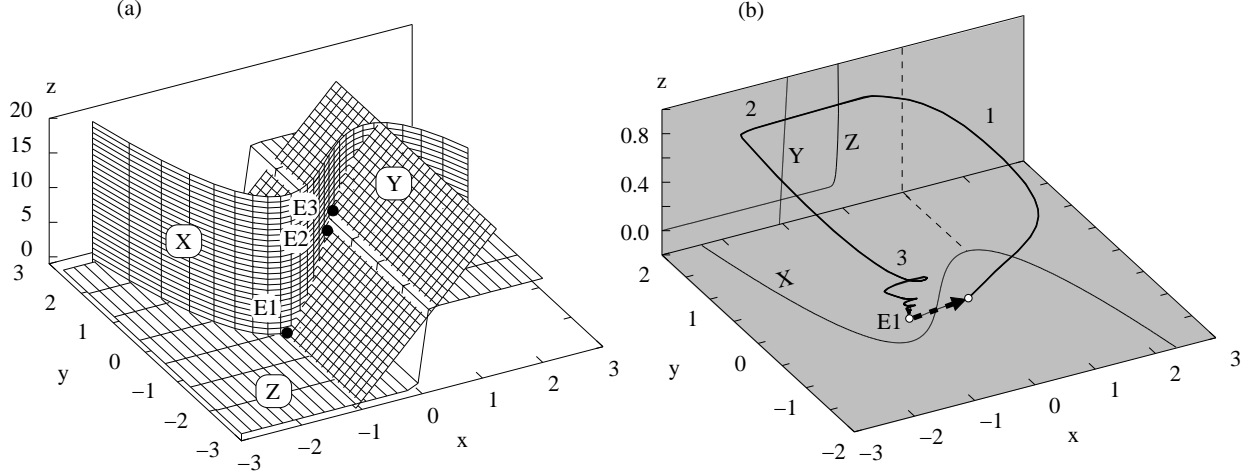


FIG. 2: (a) The 3D plot of nullclines for the FHN-K model. The intersections of the cubic x -nullcline, linear y -nullcline and sigmoidal-shaped z -nullcline may provide 3 equilibrium points. (b) shows a representative trajectory near the stable equilibrium point $E1$ (thick line). The arrow indicates the initial perturbation.

Let us look for the main features of the model in terms of the steady states and their stability. Note, at $C = 0$ our model converges back to the original FitzHugh-Nagumo model with cubic and linear nullclines and one single equilibrium point, which is stable for $|a_0| > 1$ and unstable otherwise. Including the z -dynamics the model (2)-(7) possesses three nullcline surfaces, which are depicted in Fig.2 (a) and labeled X , Y , and Z according to the equation they satisfy. One can see, that more than one intersection is possible. Namely, the condition $\dot{x} = \dot{y} = \dot{z} = 0$ gives for the steady state values x^0 :

$$x^0 + a_0 = \frac{1}{2} \frac{C\alpha}{\beta} \left(1 + \tanh\left(\frac{x^0}{x_s}\right) \right). \quad (8)$$

For such small x_s we use the right hand side of (8) is nearly a step function. Thus one fixed point can be found $x_1^0 = -a_0$, which is always stable for the parameter range we will consider. Thus the system needs over-threshold stimuli to enhance states with states $z > 0$.

Taking C as the control parameter regulating the coupling strength to the exterior variable z two additional fixed points bifurcates at a critical value C_{crit} determining from

$$\eta C_{\text{crit}} \left(1 + \sqrt{1 - \frac{2x_s}{\eta C_{\text{crit}}}} \right) - x_s \text{atanh} \left(\sqrt{1 - \frac{2x_s}{\eta C_{\text{crit}}}} \right) - a = 0 \quad (9)$$

with $\eta = \frac{\alpha}{2\beta}$.

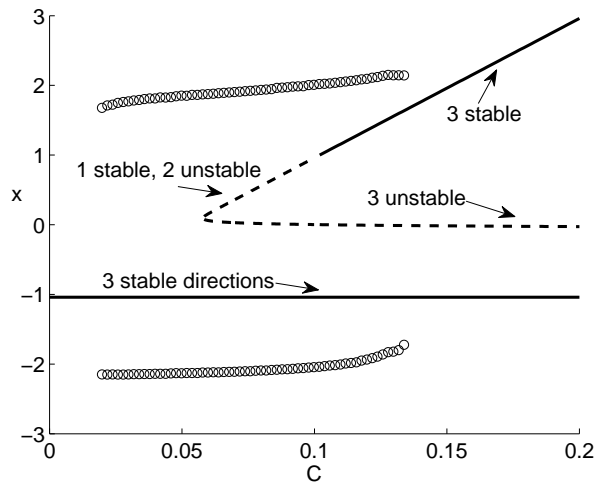


FIG. 3: bifurcation diagram for C as the control parameter. The x value of the fixed points is plotted (dashed and solid lines). Circles correspond to the extremal elongation x -values of the limit cycle.

This is depicted in fig. 3. The upper fixed point follows $x_3^0 = C\alpha/\beta - a_0$ and the corresponding z -value is the highest z -level the system can reach ($z_3^0 = z_{\max} = \alpha/\beta$). The fixed point in between is located at $x_2 \approx x_s(2\alpha\beta)/(\alpha C - 2\beta x_s)$ which is only weakly dependent on C and is unstable in every direction. In Fig.2 (a) they are labeled with $E1$, $E2$, and $E3$, respectively.

In Fig.2 (b) a representative trajectory starting in the $E1$ vicinity is shown. The nullcline surfaces are given as projections on the horizontal and vertical planes. The arrow indicates the initial perturbation that kicks the phase point from $E1$. After a super-threshold push, the trajectory quickly moves rightward, then slowly moves along the y -direction, but during this time it also moves upward approaching the z -nullcline. The vertical component of movement is defined by α . This segment is labeled with 1. Within the segment 2 of the trajectory, the vertical component changes its direction, now it moves downward controlled by β . When the phase point comes back to the vicinity of the equilibrium point, it is still raised along the z axis. From this level, the phase point moves downward with pronounced damped oscillations. Besides the fixed points there is also a parameter range where a stable limit cycle appears (see the circles in fig. 3 which indicate the extremal elongation in x for the stable periodic orbit). Initially started outside of the basin of attraction of the stable fixed points every trajectory end on that limit cycle leading to an oscillatory behavior in

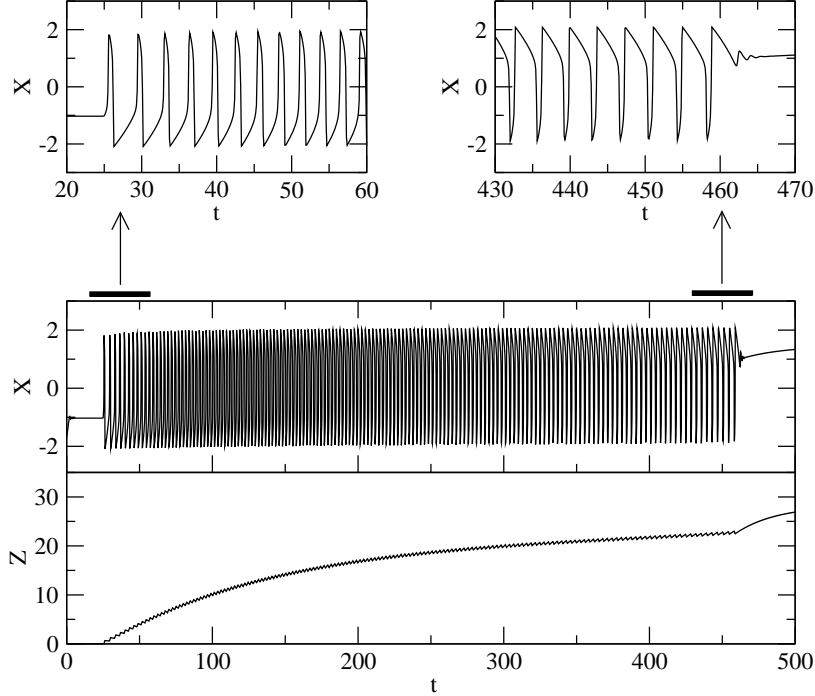


FIG. 4: Transition to the stable state at the activation state. After initiating the oscillation of x , the value of z rises and drives the system to the upper fixed point. In inserts (top row) the corresponding change of the spikes for x is illustrated. (parameters: $\tau_l = \tau_r = 1$, $\beta = 0.0354 \ll \alpha = 1.0$)

x and y and a nearly constant level of z . Due to a saddle-node bifurcation the limit cycle loses stability in one direction for too small and too high values of C . The thereby created saddle-like limit cycle annihilates with the upper fixed point $E3$ via a Hopf-bifurcation, illustrated in fig. 3 at the transition from the dashed to the solid line.

Beyond the limit cycle in a parameter range, where only the two stable fixed points exist, x and y also starts to oscillate as a long living transient when perturbing the lower fixed point initiation as depicted in fig. 4. In that case the z -level increases successively, lifting the system up to the maximal value. Thus the depolarizing spikes transform to polarization spikes, elongating from the depolarized state down to the former resting polarized level. For the selected set of parameters the level of z still increases. The inverse firing process stops and reaches the stable steady state $E3$ where neurons are embedded in extracellular space contaminated by potassium.

III. NOISY BEHAVIOR OF A SINGLE UNIT

To understand the specific features of the FHN-K model in a noisy regime, let us first consider the segment 3 of the trajectory from Fig.2 (b) in terms of the excitation threshold. Fig.5 (a) shows the time courses of the model variables at $a = 1.004$ when a short external pulse initiates the generation of a single spike. For specific values of α , the activation of z -variable is relatively fast. In the middle panel of the figure one can compare the inhibitor behavior for $C = 0.008$ (solid curve) compared with the $C = 0$ case (dashed curve). Generally, the solid curve runs lower after the spike was generated. However, there is a more complex response near the resting state.

Figure 5 (b) shows details. As we discussed above, an increased value of z evokes damped oscillations. During maxima of these oscillations the distance to values in phase space where a new excitation starts is minimal. Hence, during the moments of maximal elongation a weaker external forcing is sufficient to excite the next spike. This feature is important for the understanding how noisy input acts in this model. Namely, after a spike was produced and the refractory time is over, there are few moments of larger probability for the next noise induced firing. It resembles the behavior of so called resonate-and-fire neurons [32, 33] with subthreshold oscillations. But, differently, it occurs only after a spiking event, if still the exterior with $z \neq 0$ influences the behavior of the neuron.

The noisy behavior of model (2)-(6) is significantly controlled by the mechanism described above. For appropriate small D values the most part of noise-induced spikes appear at the first elongation after approaching the rest state as shown at $t \approx 20$ in Fig. 5 (b). There is a kind of stochastic positive feedback: once appeared, the noise-induced spiking can continue showing high regularity. If at this state current noise values were to small to override the minimized threshold, then the next spike will occurs after considerably longer time interval and noisy bursting is observed [33, 34, 35].

The described subthreshold oscillations are responsible for specific features of the averaged spectral power density $S(f)$. In the left column of Fig.6 we compare the densities of the unperturbed FHN model (case $C = 0$, given in grey) and of our model at $C = 0.03$ (2)-(6). For all panels of the figure, the noise intensity D is assumed to be small, so the noisy forcing can be regarded as weak. Both cases starts with just the same shape of $S(f)$, when only few spikes appear during the observation time (not shown in figure). In the FHN model,

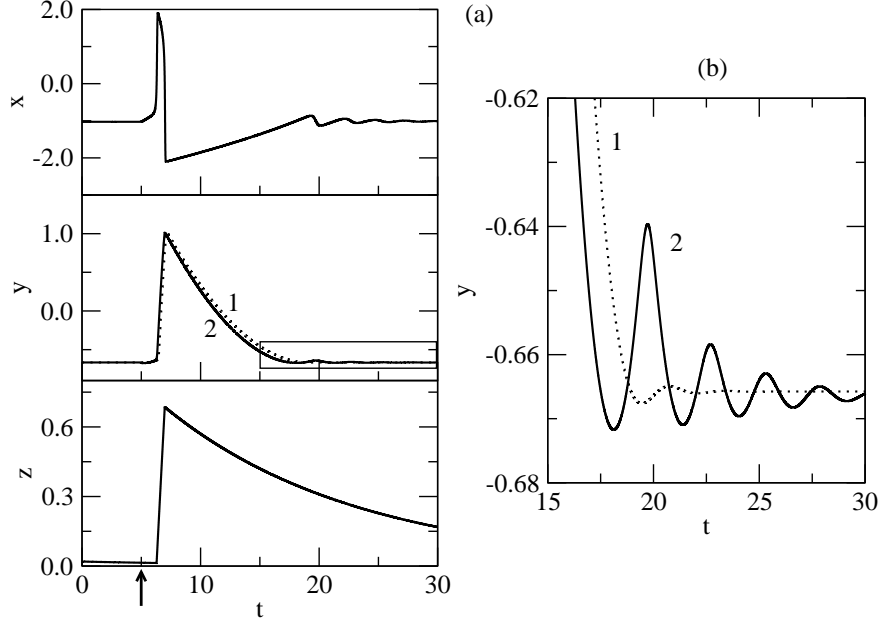


FIG. 5: (a): Temporal evolution after perturbation in the single-unit model at $C = 0.008$. The spike is initiated by a short excitatory pulse at the time indicated by the black arrow. Dotted line (1) in the middle panel shows the y -time course for $C = 0.0$. (b): the enlargement of rectangular area in (a) shows the subthreshold oscillations after spiking. The dotted (1) and solid (2) lines illustrate the cases of $C = 0.0$ and $C = 0.008$, respectively.

the further increasing of D leads to formation of a broad peak at zero frequency that moves rightward and reach the position at $f \approx 0.06$ at $D = 0.01$. It corresponds to the quite regular firing due to the effect of coherence resonance [4, 36, 37]. Model (2)-(6) shows a similar power spectrum at the very weak and at the final ($D = 0.01$) noise strength, while the evolution of the spectra with increasing noise is different. Instead of a broad peak at zero, two more sharp peaks appears at zero and at $f \approx 0.075$. The inspection of time courses shows, that the first peak corresponds to the randomly appeared bursts, while the second peak corresponds to the mean interspike distance within bursts. With increasing D , the peak at zero gradually disappears, while the peak at $f \approx 0.075$ takes more power. The third row of panels in Fig. 6 shows the considerably higher regularity of firing process in the (2)-(6) model comparing with the FHN model. The similar effect can be observed by inspecting the probability distribution density of interspike intervals (ISI) as shown in the right column of Fig. 6. While the activity near zero frequency is mapped on interval values with larger then 20.0 time units, a pronounced peak is observed at ISI values ≈ 1 which

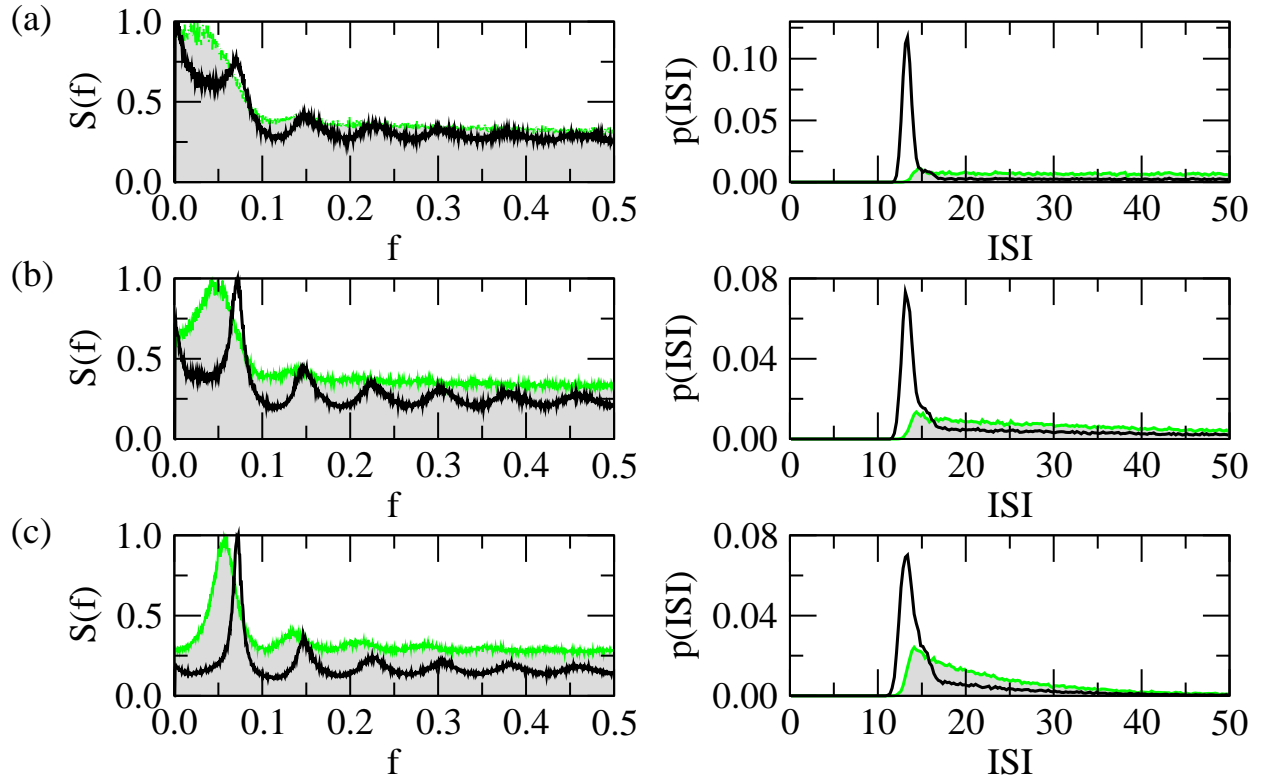


FIG. 6: (Color online) The spectral power density (left panels) and the probability distribution density of interspike intervals (right panels) for the single-unit model with noise. For comparison the maxima of the spectra are set to one. Curves in black were obtained with $C=0.03$. Curves in green with filled area were obtained with $C=0.0$ illustrating the behavior of the unperturbed FHN model. Noise intensity takes values $D=0.005$, $D=0.007$ and $D=0.01$ from top to bottom.

grows up to a optimal value with increasing intensity of noise D .

To summarize, the noisy behavior of a single excitable unit is characterized by coherence resonance and by excitation of bursting with (statistically) large intervals between groups of spike. This interesting dynamics is reflected by both the spectral power density and the ISI distribution density. The origin of this feature is what one can call a subsequent self-induced depolarization in interaction with the exterior potassium. Note, this result is consistent with previously reported behavior of higher-dimensional quantitative models [19, 20, 21]

IV. TWO EXCITABLE UNITS INTERACTING WITH A COMMON EXTERIOR

The described above self-depolarization plays an important role when two excitable cells share one $z(t)$ reservoir. Therefore the equation (7) is replaced by:

$$\dot{z} = \alpha (\Psi(x_1) + \Psi(x_2)) - \beta z, \quad (10)$$

where x_1 and x_2 belongs to the first and second unit each described by equations like (2)-(3) with the common variable z .

In such a case, firing of one unit provides depolarization for both. Figure 7a illustrates the interaction. Originally, taking separately both units are excitable, so that without external input they remain in the rest position. When a noisy stimulus or an external perturbation initiates a spike in the first unit as shown in the figure 7a, almost instantaneously the second unit becomes strongly depolarized and starts also firing with large probability. Considering the collective response, it creates a doublet, like it is shown in figure 7a at $t \in (5, 10)$. Note, that the specific time interval in which the second spike appears depends on the current values of the noisy stimulus.

If the feedback controlled by C is strong enough, a self-sustained continuous firing occurs after one of the units was excited. In this regime in case of identical units equally spaced time intervals between spikes of the first and the second units are adjusted (fig. 7b). The two units fire perfectly in anti-phase a effect which is known from glycolytic oscillations in cells [38].

Looking forward to the firing patterns in the $2D$ array of many units discussed in the next section, one can expect both: A temporal shifted firing of neighboring neurons ("one-induced-by-another" pattern) as well as a tendency to anti-phase firing of neighboring units. The latter shows a doubled frequency in the collective response.

V. NOISY DYNAMICS OF SPATIALLY EXTENDED MODELS

Coming to the extended scenario we consider an inhomogeneous medium with separated active units on the one hand and exterior modeled by z on the other hand. There are two main possibilities to construct large ensembles of coupled units in two dimensions defined by (2)-(6).

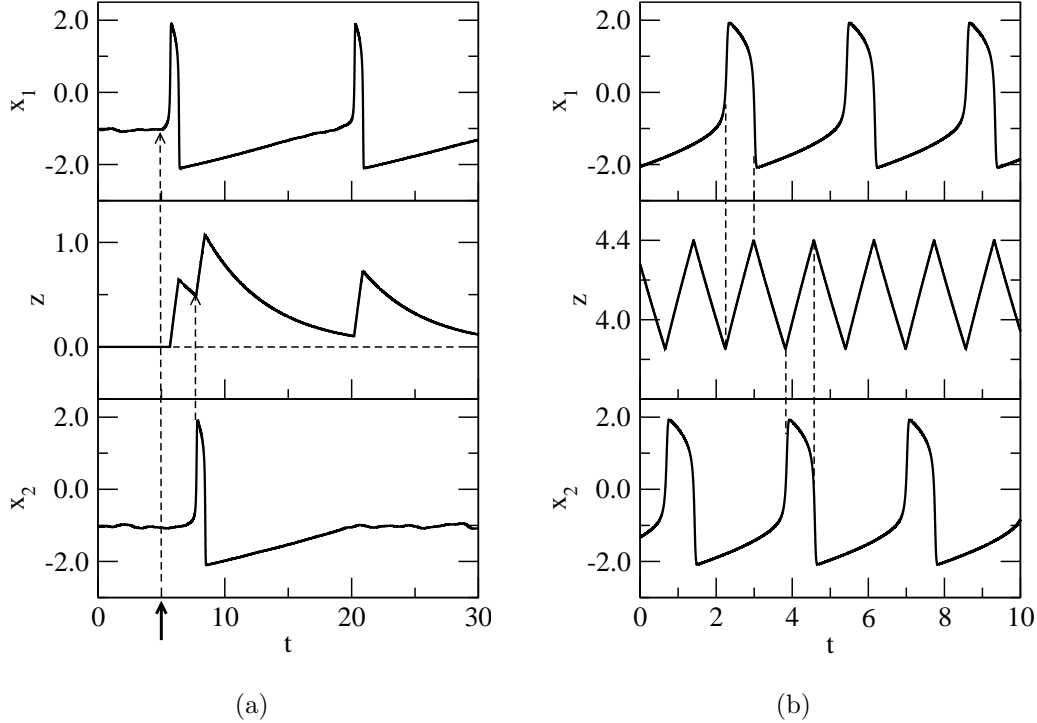


FIG. 7: Characteristic operating regimes of two coupled excitable units. Left panel: temporal evolution at weak noise. The first unit with x_1 starts firing first and provides an increase of the common external z level. It depolarizes the second unit and support its noise-induced firing. Right panel: Both units are in a oscillatory regime and show firing in anti-phase. The frequency of the common output has doubled. The limit cycle of these oscillations is in coexistence with the stable fixed point E_1 .

On the one hand we assume that the $z(\vec{r}, t)$ variable describes a continuous diffusive medium with spatial coordinates $\vec{r} = (r_1, r_2)$. The excitable units are placed in a second layer at locally separated sites coupled by the diffusing field $z(\vec{r}, t)$.

One can alternatively consider a binary medium, consisting of excitable elements embedded in the non-excitable field $z(\vec{r}, t)$, which diffuses in the remaining space of the two dimensional medium.

The first approach is evidently and leads to an usual reaction-diffusion system with three variables. Two variables are locally defined and coupled via the third. One might imagine a two layer systems with excitable units located inside a gel with low connectivity. The interaction inside this first layer can be neglected compared to the diffusive coupling of the third species $z(\vec{r}, t)$. For such mixed systems with densely packed excitable particles surrounded

by reactive emulsions pattern formation has been observed in chemical experiments [39, 40].

According to the original model of potassium mediated neuronal activity, the space is divided on cells, that are electro-chemical active surrounded of extracellular space being the diffusive medium for potassium ions. Thus, in the present work we follow the second approach. However, we also considered the two-layer system, which we will compare to the binary system giving short remarks at the following points.

In particular we use a regular array of active units in each row and column illustrated in fig. 8 following (2)-(3). For each point of the intermediate diffusive medium it holds:

$$\dot{z}_{ij} = \alpha \sum_{k \in nb_1} \Psi(x_k) + \gamma \sum_{l,m \in nb_2} (z_{lm} - z_{ij}) - \beta z_{ij}, \quad (11)$$

where the subscript ij denotes the current point in space. The second additional term describes the diffusion of the z -field with the diffusion coefficient γ . The sum indices $nb_{1,2}$ denote the sets of neighboring "neurons" and coupled units, respectively. We have implemented several types of coupling like nearest or next-nearest neighbor coupling for nb_1 and/or nb_2 . To keep it clear we discuss the results only for the coupling to the next 8 surrounding boxes, where the diagonal elements are scaled by a factor of $1/\sqrt{2}$. Taking more neighboring cells into account has no mentionable impact. Note, that in contrast to conventional reaction-diffusion systems, the active units do not interact mutually but only via the common variable z , whereas the exterior medium is locally coupled with itself and is additionally affected by the neurons activity.

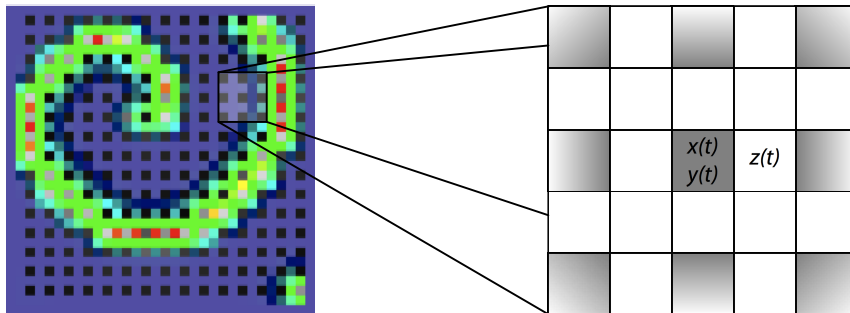


FIG. 8: (Color online) Schematic picture of the extended arrangement of neurons (N) and pure z -cells in between.

One can expect that the interplay between the refractory time of an active cell (controlled by τ_l) and the time scale of extracellular space (defined by the parameters α , γ and β in the equation for z) plays a key role in the spatial-temporal dynamics. Therefore, we have selected some representative examples that are discussed below as five trials.

Note, all the computations performed in conditions where the identical individual units possess a stable fixed point at $x^0 = -a$. We choose it as the initial condition, hence all observed operating regimes are noise induced due to the fluctuating barrier a (see eq.(4)).

The following parameters have been appointed in all cases: $\varepsilon = 0.04$, $a_0 = 1.04$, $C = 0.1$, $\tau_r = 1.0$, $x_0 = 0$, $x_s = 0.05$. Essentially only the parameters of the exterior have been set to different values according to the following table:

Parameters	α	β	γ	τ_l	D
Set #1	50.0	6.0	2.0	1.5	0.00005
Set #2	60.0	6.0	130	1.5	0.02
Set #3	6.0	0.35	4.0	1.5	0.0001
Set #4	10.0	0.6	0.2	2.0	0.00002
Set #5	150.0	6.3	2.0	1.5	0.003

With the increasing set number the mean z -level rises successively corresponding to a growing value of the coupling parameter C . According to the bifurcation diagram fig. 3 we go to the right along the abscissa and encounter excitable, oscillatory and bistable behavior. We underline that the rest state of the uncoupled FHN is always a stable homogeneous state of our dynamics with $z = 0$. Excitations of spatio-temporal structures need over-threshold noisy stimuli or corresponding initial conditions.

Set #1. Waves, Spots and Spirals (Fig. 9)

The local dynamics is excitable. By noise the units can be activated and release z to their neighborhood. In this case the outside concentration of the medium decays much faster than the units recover, while the diffusion is too slow to distribute the delivered z over a large distance.

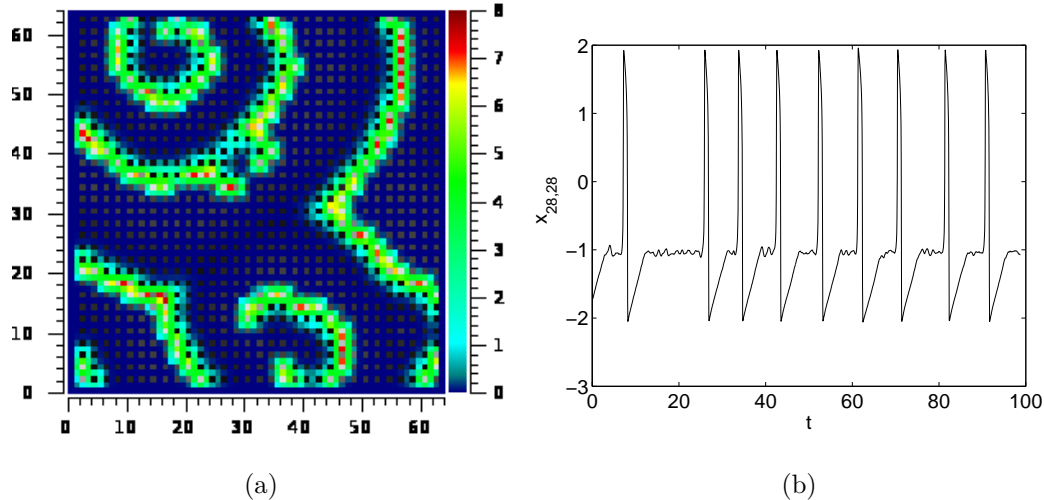


FIG. 9: (Color online) parameter set #1: (a) Noise induced spirals and wave fronts. The colorbar indicates the z -level whereas white and black represents active cells in the excited and rest state respectively. (b) Time series of an arbitrary chosen cell.

The units that crossed over in the refractory period ignite other neighboring units via the medium and a traveling noise-supported extended waves is excited as it is depicted in fig. 9(a).

At the system borders or due to noise circular waves can break and the free endings curl to form a spiral wave. Although the dynamics is purely excitable at the chosen noise intensity waves appear very regularly, noticeable in the time series of fig. 9(b). The mean firing rate of the active cells is $r_{mean} \approx 0.1$ and the mean exterior concentration is $z_{mean} \approx .8$.

The combination of the chosen diffusion $\gamma = 2.0$ with considerable refractory time of neurons stabilizes the location of the center of noise-induced spiral wave in spite of all units receive random stimulus of the same intensity. One may eliminate in the dynamics the z -variable which would reduce the system of equations to two components standing for a single activator x and inhibitor y . Compared to the usual case the coupling term (diffusion of activator) appears in the equation of the inhibitor, similar to a Soret effect. Slightly increased noise strength destroys the spiral wave structure by splitting it into short fragmented traveling waves that nucleate and annihilate in a random manner.

The release of potassium in the exterior is still sufficiently low and so far no new fixed point bifurcates at high z -values. Therefore the background in the large refractory state relaxes always to small z - values as indicated by the dominating blue color in the figure.

In the two-layer system only for a decay rate of $\beta \approx 4$ or smaller, noise supported short living wave segments appear.

Set #2. Noise supported traveling clusters (Fig. 10)

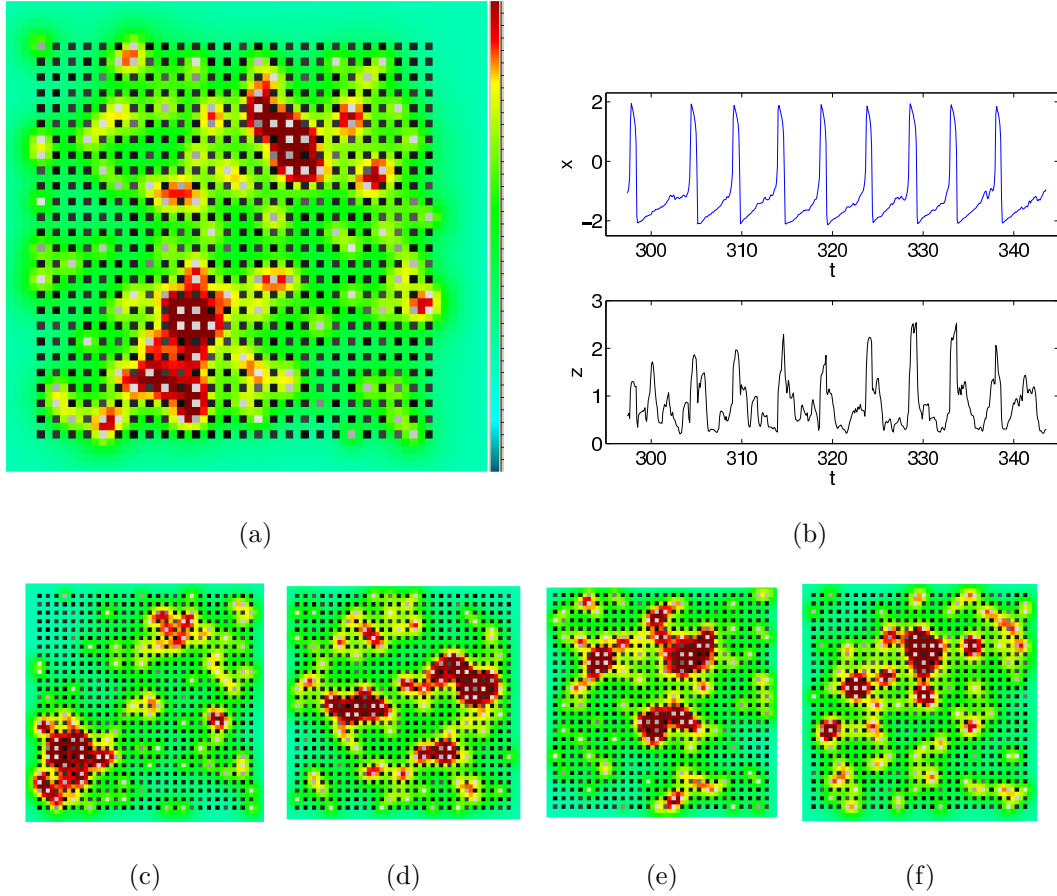


FIG. 10: (Color online) parameter set #2, Colors like in fig. 9(a) self-feeding clusters. (b) Time series of an arbitrary chosen cell and of an neighboring z -cell. (c)-(f) snapshots of nucleating, wandering and decaying clusters

The pronounced difference to the former set of parameters is the very large z -diffusion coefficient γ and the high noise level. Nuclei that would lead to coherent patterns like spirals diffuse very fast forming still connected clusters of delivered z . Such developed clusters can live relatively long wandering through the medium due to the noisy forcing.

The local dynamics is excitable and possess only the lower fixed point as a steady state. Due to the fast z -diffusion a large vicinity of units gets activated whenever one is excited

which supports the formation of a localized high-level z region. Inside those areas the threshold of the units is lowered and the release of z increases. This process leads to self-feeding meandering cluster as depicted in the snapshots of fig. 10(c-f).

Note, that noise is necessary over the whole time to keep the clusters alive. Switching the noise off lead to a complete decay of the z -level to zero. For the given noise intensity the stochastically occurring spikes events are quite regular. The z -level follows the activation and forms also coherent oscillation-like elongation as shown in fig 10b. The mean rate is $r_{mean} \approx 0.2$ and the mean z -concentration is $z_{mean} \approx 1.0$.

Set #3. Desynchronized oscillators embedded in a z -sea (Fig. 11)

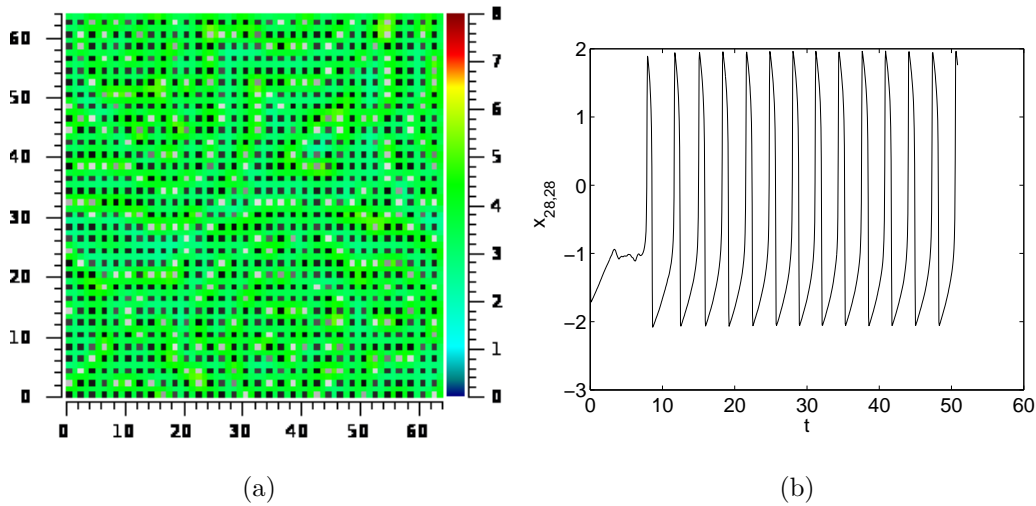


FIG. 11: (Color online) parameter set #3: (a) Elevated z -level due to permanently oscillating active cells.. Colors like in fig. 9(a). (b) Time series of an arbitrary chosen cell.

Compared to the former case less potassium is released but it is also slower decaying. The refractory time is short $\tau_l = O(1)$ compared to the decay time β^{-1} and therefore we observe oscillating units (fig. 11b) embedded in a situation that high z values survive longer than the duration of one oscillation period. Thus the exterior is permanently fed by potassium which is diffusing over long distances, shown in fig. 11(a).

Starting at the $z = 0$ level, the active units first perform the noise induced transition to the oscillatory behavior. Except for the the initiating perturbation noise is not needed to keep the oscillation alive. All units moves along the limit stable cycle but with different

phases. Along such sites the medium is fast filled with z which starts to propagate elevating the neighborhood and forming a front like spread over the space. It is a typical scenario of nucleation in systems with multiple attractors.

Despite that a second attractor at high z -values exists it will never be reached due to the decay rate β which is still high enough to compensate the release rate α . Thus a quasi-steady picture remains with a sea of high potassium populated by active units blinking regularly and feeding the exterior with potassium. Here, we find for the oscillation frequency $r_{mean} \approx 0.34$ and for the mean exterior $z_{mean} \approx 5.7$.

Two times larger α and β and 20 times smaller diffusion originates another similar pattern: after some transient, high z -concentration occupies all available space. After that, a noise-induced neuronal firing moving as complex pattern through the medium. A detailed inspection shows that the observed behavior is locally based on the anti-phase firing of neighboring units inside the constant sea of high z -level. In 2D space it produces a chess-like firing pattern, when all neighbors fire in anti-phase. In the deterministic case it forms regular phase waves moving from borders to the center. Noise adds irregularity and evokes many additional patterns.

In figure 13a the spatial correlation function is shown for an arbitrary neuron over the distance to its neighboring excitable units along a row. The solid line represents the long range correlation to the active units in the neighborhood, when the noise has not yet disturbed the wave-like propagation of the stimulus that lifts the units to the limit cycle.

A slow decay of the correlation is shown expressing the indirect diffusive coupling. The first dip corresponds to the next nearest neuron which is less correlated to the considered unit than the next but one. It reflects that on average neighboring elements can fire preferable in antiphase.

However, a small amount of noise will drive the system to a complete desynchronized state after a couple of oscillations, shown as the dashed line in fig. 13a

The described situation is typical for the studied extended system and can be found over a large parameter range. Also in the two-layer system the same oscillating regime exists for the same parameter set.

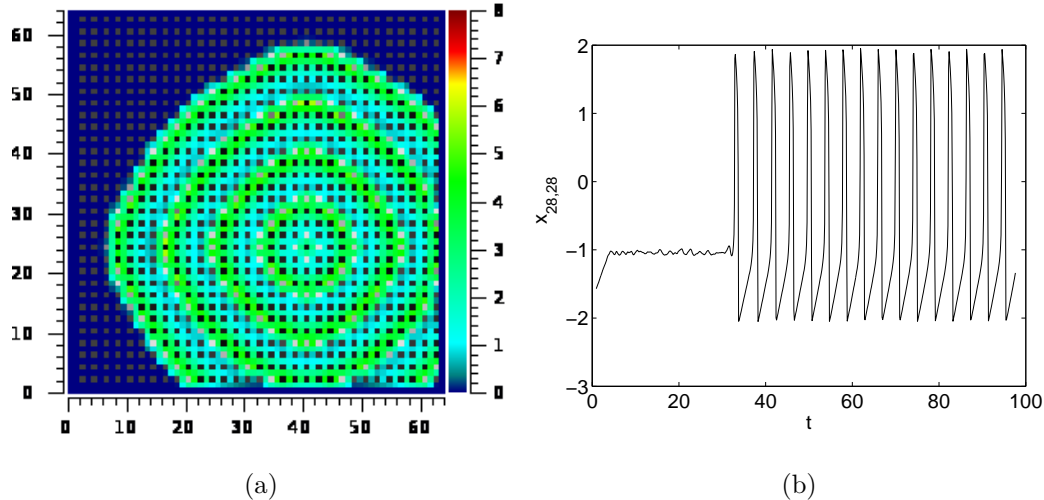


FIG. 12: (Color online) parameter set #4: (a) Noise induced concentric waves. Colors like in fig. 9(a). (b) Time series of an arbitrary chosen cell.

Set #4. Oscillations form a propagating ring-like pattern (Fig. 12)

Similar to the former parameter set, a single cell, fluctuating around the rest state, can reach the stable limit cycle, we mentioned above, by overcoming the unstable limit cycle due to noise. At this noise level those events are rare. Once happened β is so small, that the z -level around the oscillating cell can rise and reach the next cells without decaying before. Therefore all active units can be elevated to the oscillatory behavior successively and a concentric wave appears, shown in fig. 12(a). A typical time series of x recorded from a single cell is depicted in fig. 12(b). For the chosen parameters the oscillation period after the transition is $r_{mean} \approx 0.25$, while the z -level averages $z_{mean} \approx 6.0$. Compared to the last case diffusion of potassium is reduced drastically. It gives reason that spatial structure can establish at length scale of a few neurons.

The wavelength is represented in the spatial correlation shown in fig. 13b, where the solid line shows a long range correlation shortly after initiating the wave pattern. The active units are well synchronized and noise needs longer to destroy the structure (dashed line in fig. 13b).

Increasing β the stable and unstable limit cycle annihilate and the local dynamics is excitable. A noise induced super-threshold perturbation leads to a singular depolarization of the active cell and the z -level in it's neighborhood increases. Thus the next cell becomes

depolarized as well and singular a ring-like wave emerges.

Further increase of β allows only a small neighborhood of the initially activated cell to get enough released z . However, such activated wave segments can be stable for a long time while traveling through the medium.

This kind of patterns always decay in the two-layer situation. The released z can diffuse to each site of the array without restriction. So the release rate α need to be higher For example choosing $\alpha = 15$ and a big enough initial nucleus an oscillon is formed. This structure is an extended but localized spot fed by oscillating cells inside and surrounded by inactive cells.

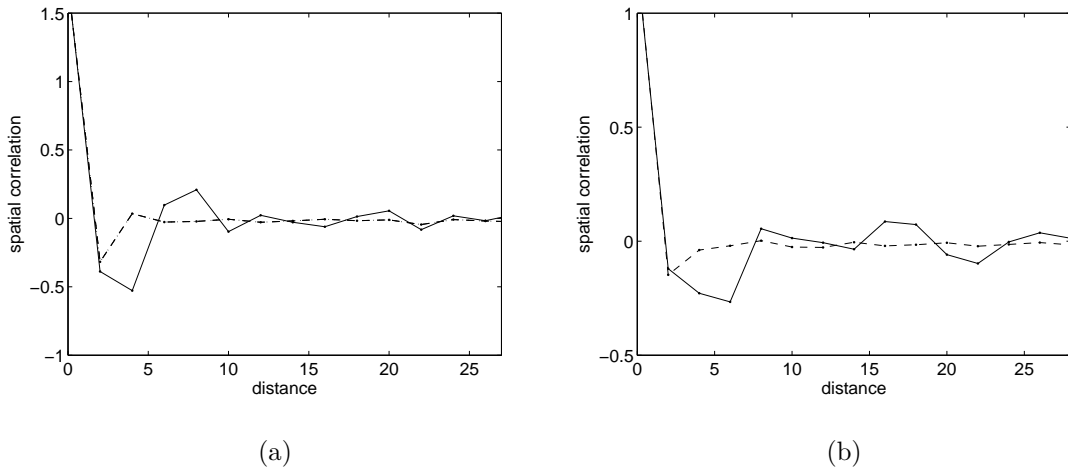


FIG. 13: The spatial correlation of set #3 (left) and set #4 (right) over the distance exclusively to neighboring neurons is shown. Solid lines indicates transient behavior for early times, dashed lines show the mixed system due to noise.

Set #5. Bistability and inverted waves. (Fig. 14)

Fig. 14 illustrates the case of the highest release rate α , considered here.

After the nucleation of a bistable wave all the space becomes initially occupied by the high-level z spot ($z = 24$) which is stable due to the bifurcation of a second stable fixed point at the depolarized state of the cells. Thus the vicinity of the activated cells is permanently filled with z dissipated with β and diffusively distributed with γ .

An inverse situation occurs. Noise can create low level patterns, like inverted spirals or propagating waves shaped into the high-level z sea. Depending on the noise configuration

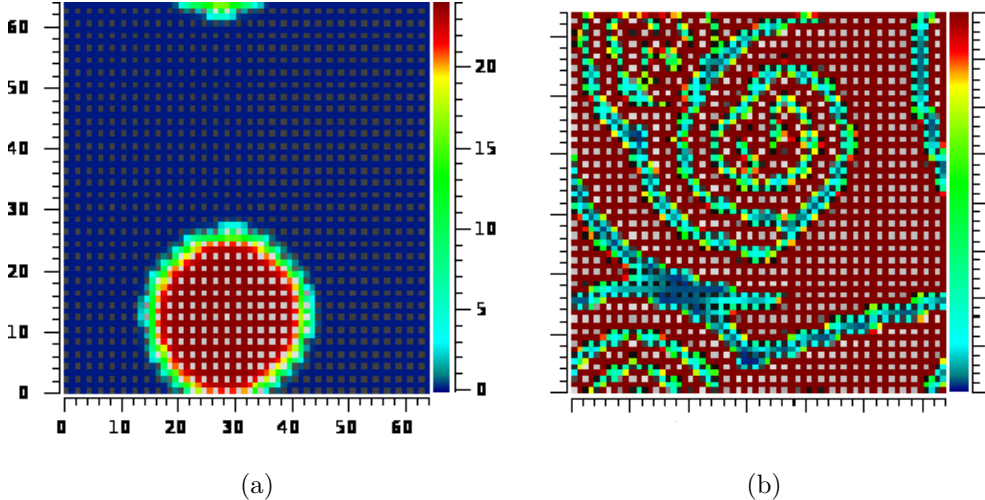


FIG. 14: (Color online) parameter set #5: (a) A bistable wave covers the medium with the high-level z state. Colors like in fig. 9(a). (b) Noise induced inverted spirals and waves. The scales are the same like in (a).

it is also possible, that the system reaches the $z = 0$ state again by the appearance of the inverted bistable front.

Such coherent patterns doesn't exist in the vicinity of the considered parameters for the two-layer system, after the high-level z state is reached. Only independent break-ins are taking place stochastically.

From the dynamical point of view, the existence of such a regime can be explained as follows. The considerable elevation of z shifts the operation point of core FHN model to the opposite side of the cubic nullcline. Operating on the background of high exterior z and corresponding to the shifted fixed point, each subthreshold perturbation leads to an inverted spike being the impulse from resting high level to the low one. Now τ_r controls the duration of an anti-spike while τ_l define the refractory time (Fig. 14b) The above described mechanism is already discussed in Fig. 4 for a single active unit having two stable steady states.

VI. CONCLUSIONS

In this paper we have introduced a model that qualitatively describes the neuronal dynamics at variable extracellular concentration of potassium ions. Using the FitzHugh-Nagumo

model as prototype for an excitable unit, we added a pathway that qualitatively takes into account the potassium release from the neurons and the depolarization (threshold lowering) as a result of the increased extracellular potassium level.

The analysis of the model for a single unit, for two coupled units, as well as for an extended array have shown that:

- (i) The stochastic model of a potassium driven excitable neuron exhibits bursting as the firing pattern. Its due to subthreshold oscillations for higher values of potassium. As a result, the power spectrum with increasing intensity differs from the typical one for an excitable system with strong time scale separation. It shows a more pronounced and narrow peak at a frequency different from zero. The broad peak gradually close to zero-frequency disappears with growing noise intensity.
- (ii) In the excitable regime two potassium-coupled neurons being forced by noise show doublets of spikes. Firing of one neuron strongly depolarizes the second neuron and makes its firing almost inevitable. In many cases these doublets tend to an oscillatory behavior being synchronized in anti-phase and possessing a frequency doubled to the spiking of a singular neuron.
- (iii) A two dimensional array of potassium-driven neurons shows a variety of noise-induced spatial-temporal firing patterns depending on the relation between the characteristic timescales of the model and the noise intensity. One of the most interesting patterns is the long-living randomly-walking spots. Another effect is the high-level potassium state with inverted spots being the result of the medium-driven shift of equilibrium state toward the right part of cubic nullcline.

In spite of simplicity of the generalized model we use, some links can be made between our results and relevant neuro-physiological studies. Namely, the well known but still debating 'potassium accumulation hypothesis' [22, 41, 42] considers the self-sustained rise of extracellular potassium as the cause of epileptiform activity. Taking it in mind, our computational results can be classified as following: the short-term activation of z -medium (including concentric and running waves) might describe the potassium dynamics within the physiological range, while the patterns with persistent high level of z variable resemble the formation of epileptic seizure and thus can be regarded as representing pathological conditions. Thus,

an interesting future work can be done to reveal the possibility and conditions for mutual transitions between 'normal' and 'pathological' states.

We thank S. Rüdiger (Berlin) for fruitful discussion and cooperation. D.P. acknowledges the support from RFBR grant 09-02-01049. F.M. and L.S.G. acknowledges the support by the SFB 555 and R.B. Schuppner thanks for support by the Bernstein Center for Computational Neuroscience.

-
- [1] Hodgkin A.L., Huxley. A.F., J. Physiol. London, **117**, 500-544 (1952).
 - [2] Keener J. and Sneyd J., *Mathematical Physiology* (Springer, New York) (1998).
 - [3] FitzHugh R.A., Biophys. J. **1**, 445 (1961).
 - [4] Lindner B., Garcia-Ojalvo J., Neiman A.B., and Schimansky-Geier L., Phys. Rep.392, 321 (2004).
 - [5] Sykova E. Prog. Biophys. Mol. Biol. **42**, 135 (1983).
 - [6] Dahlem Y.A., Dahlem M.A., Mair T., Braun K. and Müller S.C., Exp. Brain Res. **152**, 221 (2003)
 - [7] Yi C.-S., Fogelson A.L., Keener J.P. and Peskin C.S. **220**, 83 (2003).
 - [8] Yan G.X., Chen J., Yamada K.A., Kleber A.G. and Corr P.G. J.Physiol. **490**, 215 (1996).
 - [9] Hansen A.J. Acta Physiol. Scand. **102**, 324 (1978).
 - [10] Cressman J.R. Jr., Ullah G., Ziburkus J., Schiff S.J. and Barreto E. J. Comput Neurosci **26**, 159-170 (2009).
 - [11] Ullah G., Cressman J.R., Barreto E. and Schiff S.J. J. Comput Neurosci **26**, 171-183 (2009).
 - [12] Deitmer J.W. , Rose C.R., Munsch T., Schmidt J. , Nett W. , Schneider N.-P. and Lohr C. , Glia **28**, 175-182 (1999).
 - [13] Bazhenov, M., Timofeev, I., Steriade, M. and Sejnowski, T.J., Journal of Neurophysiology **92**, 1116-32 (2004).
 - [14] Park E-H. and Durand D.M., Journal of Theoretical Biology **238**, 666-682 (2006).
 - [15] Vern B.A., Schuette W.H., Thibault L.E., J Neurophysiol 40(5):1015-23. (1977)
 - [16] Gardner-Medwin A.R. J Physiol 335:393-426,(1983).
 - [17] Odette L.L., Newman E.A. Glia 1(3):198-210, (1988).
 - [18] Dietzel I., Heinemann U., Lux H.D. Glia 2(1):25-44. (1989).

- [19] Kager H., Wadman W.J., Somjen G.G.. J Neurophysiol 84(1):495-512 (2000).
- [20] Kager H., Wadman W.J., Somjen G.G.. J Neurophysiol 88(5):2700-12, (2002).
- [21] Fröhlich F., Bazhenov M., Timofeev I., Steriade M., Sejnowski T.J. J Neurosci 26(23): 6153-62, (2006).
- [22] F. Fröhlich, M. Bazhenov, V. Iragui-Madoz and T. J. Sejnowski, Neuroscientist 14 422 (2008).
- [23] Postnov D.E., Ryazanova L.S., Sosnovtseva O.S., Mosekilde E., Journal of Neural Systems**16**, 99-109 (2006) .
- [24] Postnov D.E., Ryazanova L.S.,Zhirin R.A. , Mosekilde E. and Sosnovtseva O.V., International Journal of Neural Systems, Vol. 17, No. 2 (2007) 105-113
- [25] Timofeeva Y. and Coombes S. , Phys. Rev. E **68**, 021915 (2003).
- [26] Timofeeva Y., Lord G.J. and Coombes S. , Neurocomputing **69**, 1058-1061 (2006)
- [27] Berenstein I. ,Dolnik M. ,Yang L., Zhabotinsky A.M. and Epstein I. R.: Phys. Rev. E **70**, 046219 (2004).
- [28] Taylor A. F. , Tinsley M. R. , Wang F., Huang Z. and Showalter K.: Science **323** 614-617 (2009)
- [29] Falcke M. 2003 New J. Phys. **5** 96 .
- [30] Shuai J.W. and Jung P. , Phys. Rev. E **67**, 031905 (2003).
- [31] Radehaus C., Dohmen R., Willebrand H. and Niedernostheide F.-J., Phys. Rev. A **42**, 12 (1990).
- [32] Izhikevich E.M. Neural Networks J. **14**,883-894 (2001).
- [33] Verechtchaguina T., Schimansky-Geier L., and Sokolov I. M., Phys. Rev. E **70**, 031916 (2004).
- [34] Schwalger T. and Schimansky-Geier L., Phys. Rev. E **77**, 031914 (2008).
- [35] Lacasta A. M., Saguès F., and Sancho J. M., Phys. Rev. E **66**, 045105 (2002).
- [36] Pikovsky A.S., Kurths J., Phys. Rev. Lett. **78**, 775-778 (1997).
- [37] Han S.K., Yim T.G., Postnov D.E., and Sosnovtseva O.V., Phys. Rev. Lett. **83**, 1771 (1999).
- [38] Wolf J. and Heinrich R., BioSystems **43**, 1-24 (1997).
- [39] Epstein I. R., Vanag V. K., Chaos **15**, 047510 (2005).
- [40] Tinsley M. R., Taylor A. F., Huang Z. and Showalter K., Phys. Rev. Lett. **102** 1583301 (2009).
- [41] Green .J.D., Physiol. Rev. 44:561-608.(1964).
- [42] Fetziger A.P., Ranck J.B. Jr. Exp. Neurol. 26(3):571- 85 (1970).